Eidgenössische Technische Hochschule Zürich

Ecole polytechnique fédérale de Zurich
Politecnico federale di Zurigo
Swiss Federal Institute of Technology Zurich

A Scale-Residual Model for Large-Eddy Simulation

J. Maurer and M. Fey

Research Report No. 99-06
April 1999

Seminar für Angewandte Mathematik
Eidgenössische Technische Hochschule
CH-8092 Zürich
Switzerland

A Scale-Residual Model for Large-Eddy Simulation

J. Maurer and M. Fey

Seminar für Angewandte Mathematik
Eidgenössische Technische Hochschule
CH-8092 Zürich
Switzerland

Research Report No. 99-06 April 1999

Abstract

A subgrid-scale model for large-eddy simulation is developed and a conservative formulation of the filtered compressible Navier-Stokes equations is derived. We introduce a different way of looking at LES modelling: In contrast to other approaches, which estimate the subgrid-scale quantities explicitly out of the instantaneous filtered solution, the residual between the time evolution of two solutions of the Navier-Stokes equations (without a model) on different grids will be used to construct the model. Hence, no subgrid values are calculated explicitly but only their influence on the resolved scales is modelled. By this approach most of the physical information already included in the Navier-Stokes equations will be retained and less additional physical information about the turbulent flow has to be inserted.

1 Introduction

An important issue in large-eddy simulation (LES) is the clear distinction between grid-scales (GS) and subgrid-scales (SGS). The former are resolved on the numerical grid, the latter are missing in the numerical flow field and their effect on the resolved scale motions has to be described by a so-called SGS model. The definition of GS and SGS was given in the work of Leonard [7], where he introduced the concept of filtering in space. The filtering is a convolution of the variables $f(\vec{\mathbf{x}}, t)$ with a filter function F

$$\mathcal{F}f \equiv \overline{f(\vec{\mathbf{x}}, t)} = \int_\Omega F(\vec{\mathbf{x}} - \vec{\mathbf{y}}; \Delta) f(\vec{\mathbf{y}}, t) d\vec{\mathbf{y}} \tag{1}$$

where Δ is a length scale that defines the filter width and $\mathcal{F}$ denotes the filter operator. To ensure the conservation of the filtered variables it is necessary to impose the normalisation condition

$$\int_\Omega F(\vec{\mathbf{x}}) d\vec{\mathbf{x}} = 1 \ .$$

The variable f can now be written as a sum of the filtered grid-scale and residual subgrid-scale part $f = \overline{f} + f'$. Also the filtering and differentiation commute for a constant filter width

$$\overline{\frac{\partial f}{\partial x_i}} = \frac{\partial \overline{f}}{\partial x_i} \ .$$

This property is essential for LES because it allows to obtain the Navier-Stokes equations for the filtered variables. For this reason the commutivity will always be used even if it is not valid! An investigation into this commutation error and its reduction to a term of order $O(\Delta^2)$ can be found in [11]. However, the filtering does not commute with the non-linear terms of the Navier-Stokes equations. This leads to the modelling terms in the LES formulation, which contain the fluctuations between the GS and SGS part. In general these terms are estimated out of the instantaneous filtered solution. In section 2 we will introduce a different approach where the model can be constructed out of the commutation error of two different time evolutions of the solution.

When dealing with compressible Navier-Stokes equations it is convenient to introduce the Favre average

$$\tilde{f} = \frac{\overline{\rho f}}{\overline{\rho}}$$

to decouple the filtered terms $\overline{\rho f}$. This decoupling fails for the filtered product

$$\overline{\rho f g} = \overline{\rho}\widetilde{fg} = \overline{\rho}\tilde{f}\tilde{g} + \overline{\rho}(\widetilde{fg} - \tilde{f}\tilde{g})$$

because the last term on the r. h. s. can not be evaluated out of the filtered quantities and has to be modelled. By applying the filter to the Navier-Stokes equations we obtain the equations for the GS quantities

$$\mathbf{U}_t + \nabla \cdot \underline{\mathbf{F}} = \nabla \cdot \underline{\mathbf{G}} + \nabla \cdot \underline{\mathbf{H}}, \tag{2}$$

with

$$\mathbf{U} = \begin{pmatrix} \overline{\rho} \\ \overline{\rho}\tilde{\vec{\mathbf{u}}} \\ \overline{\rho}\tilde{E} \end{pmatrix}, \quad \underline{\mathbf{F}}(\mathbf{U}) = \mathbf{U}\tilde{\vec{\mathbf{u}}}^T + \begin{pmatrix} \mathbf{0}^T \\ \underline{\mathbf{I}} \\ \tilde{\vec{\mathbf{u}}}^T \end{pmatrix} \overline{p}\,,$$

$$\underline{\mathbf{G}}(\mathbf{U}, \nabla\mathbf{U}) = \begin{pmatrix} \mathbf{0}^T \\ \underline{\overline{\tau}} \\ \overline{\vec{\mathbf{u}}^T \underline{\tau}} + \overline{\kappa(\nabla T)^T} \end{pmatrix}, \; \underline{\mathbf{H}}(\mathbf{U}) = -\overline{\rho} \begin{pmatrix} \mathbf{0}^T \\ \underline{\sigma} \\ \mathbf{K}^T + c_p \overline{\rho} \mathbf{Q}^T \end{pmatrix}$$

and $\underline{\tau} = \rho\nu\left(\nabla\vec{\mathbf{u}} + (\nabla\vec{\mathbf{u}})^T - \frac{2}{3}\underline{\mathbf{I}}\nabla\cdot\vec{\mathbf{u}}\right)$. The terms in $\underline{\mathbf{H}}$ contain the fluctuations between the GS and SGS part and have to be modelled:

$$\underline{\sigma} = \left(\widetilde{\vec{\mathbf{u}}\vec{\mathbf{u}}^T} - \tilde{\vec{\mathbf{u}}}\tilde{\vec{\mathbf{u}}}^T\right), \mathbf{K} = \left(\widetilde{k\vec{\mathbf{u}}} - \tilde{k}\tilde{\vec{\mathbf{u}}}\right), \mathbf{Q} = \left(\widetilde{T\vec{\mathbf{u}}} - \tilde{T}\tilde{\vec{\mathbf{u}}}\right)$$

with

$$k = \frac{\vec{\mathbf{u}}^T\vec{\mathbf{u}}}{2}\,.$$

For the equation of state we obtain

$$\overline{p} = (\gamma - 1)\overline{\rho}\left(\tilde{E} - \tilde{k}\right) = \overline{\rho}R\tilde{T}\,.$$

By this approach $\overline{\rho}\tilde{E}$ is the total energy so that the Navier-Stokes equations are in conservation form. However, $\tilde{k}$ cannot be obtained from the filtered variables directly so that the conservation form of the equations will normally be given up either by considering only an equation for the temperature or neglecting the fluctuations of the kinetic energy in $\overline{\rho}\tilde{E}$ following the arguments of [4] or [8]. Yet, this energy is not a conserved quantity anymore and as mentioned in [4] the assumptions for the simplification are not

always fulfilled. Here the total energy is used and in order to determine $\tilde{k}$ an additional equation for the subgrid kinetic energy is introduced

$$\overline{\rho}\hat{k} = \overline{\rho}\left(\tilde{k} - \frac{\tilde{\vec{\mathbf{u}}}^T\tilde{\vec{\mathbf{u}}}}{2}\right) \ .$$

Hence, the equation of state can be evaluated and the system is closed. The equation for $\overline{\rho}\hat{k}$ can be derived from the Navier-Stokes equations

$$(\overline{\rho}\hat{k})_t + \nabla\cdot(\overline{\rho}\hat{k}\tilde{\vec{\mathbf{u}}}) + \nabla\cdot(\overline{\rho}\mathbf{K}^T) + \overline{\vec{\mathbf{u}}^T\nabla p} - \tilde{\vec{\mathbf{u}}}^T\nabla\overline{p} = \overline{\vec{\mathbf{u}}\cdot\nabla\cdot\underline{\tau}} - \tilde{\vec{\mathbf{u}}}\cdot\nabla\cdot\overline{\underline{\tau}} + \mathsf{s} \quad (3)$$

where s is a source term which has been introduced additionally and will be defined in section 2.2. It is obvious that this equation is not in conservation form, but $\overline{\rho}\hat{k}$ only occurs in the equation of state and does not affect the conservative property of the Navier-Stokes equations.

In order to solve the system the unknown subgrid values $\underline{\mathbf{H}}$ have to be modelled. In general this term is estimated out of the instantaneous filtered solution. Hence, $\underline{\mathbf{H}}$ depends on the filtering operation, but for most LES models one assumes that this coupling is very weak and applies the filter and model independently. Nevertheless, a dependence of the solution on the type of the filter has been observed, cf. [12] and the "deconvolution" models are directly based on this coupling, because here, an inverse of the filter operator is constructed to estimate the unresolved quantities.

Most LES models separate the formulation of the LES problem from the numerical method used to solve the filtered Navier-Stokes equations. However, numerical viscosity will be introduced which contributes to the model and hence contradicts this assumption. The monotone integrated large-eddy simulation approach (MILES) in [1] even suggests that no explicit SGS modelling is necessary for this algorithm and the numerical viscosity is sufficient to describe the energy dissipation. It is clear that the subgrid values will not be computed explicitly but only their influence on the resolved field is modelled. This close coupling has some drawbacks. The numerical viscosity strongly depends on the numerical scheme, its approximation order and the grid topology, so that the model also changes with these parameters and it is not clear if the variation of the numerical viscosity coincide with the model term. On the other hand, the model produces reasonable results for the GS motion which indicates that the numerical contribution to the model term cannot just be neglected and should be incorporated into the SGS model.

2 Scale-residual model

In [2] it has been shown that the solutions of the Navier-Stokes equations are quite stable to perturbations within the inertial range but are unstable to perturbations of the lowest modes, which indicates that the concept of LES is reasonable. Furthermore, for homogeneous turbulent flows they observed that the high wave-number information can be recovered almost completely if some low modes are known exactly over time and the high modes are obtained by solving for all wave-numbers. In other words, the number of degrees of freedom of a turbulent solution seems to be much smaller than one expects out of the resolution requirements for a DNS. As a conclusion from this result, a LES model should have information about the history of the low modes. Unfortunately, this information is not available in general.

We consider the non-filtered Navier-Stokes equations which can be formally written as

$$\mathbf{V}_t = \mathcal{N}\mathbf{V}$$

where $\mathcal{N}$ is a nonlinear operator and $\mathbf{V}(\vec{\mathbf{x}}, t)$ an exact solution. In LES only the filtered solution is known and a modified operator $\mathcal{M}$ which describes the model term $\nabla \cdot \underline{\mathbf{H}}$ has to be used to approximate the exact solution

$$\mathcal{F}(\mathbf{V})_t \approx (\mathcal{F}\mathbf{V})_t = \mathcal{M}(\mathcal{F}\mathbf{V}) \; .$$

The modified operator $\mathcal{M}$ can be split into the operator for the non-filtered Navier-Stokes equations $\mathcal{N}$, henceforth standard operator, and a model operator $\mathcal{H}$

$$\mathcal{M} = \mathcal{N} + \mathcal{H} \; . \tag{4}$$

Clearly, the constraint on the operator $\mathcal{H}$ is to minimise the error between the exact and modelled solution, i. e. it has to have a minimal influence on the low modes of the exact solution. Using (4) the error reads

$$\mathbf{E} = (\mathcal{F}\mathcal{N} - \mathcal{M}\mathcal{F})\mathbf{V} = ((\mathcal{F}\mathcal{N} - \mathcal{N}\mathcal{F}) - \mathcal{H}\mathcal{F})\,\mathbf{V} \; .$$

The model operator has to compensate the error which has been introduced by applying the standard operator to the filtered solution. $(\mathcal{F}\mathcal{N} - \mathcal{N}\mathcal{F})$ is therefore the "exact" modelling term. The new model uses this term directly to obtain the model operator. If we filter the LES operator explicitly so that $\mathcal{N}\mathcal{F}\mathbf{V}$ becomes $\mathcal{F}\mathcal{N}\mathcal{F}\mathbf{V}$ we can write the model operator as

$$\mathcal{F}\mathcal{H}\mathbf{V} = (\mathcal{F}\mathcal{N}(\mathcal{F}_K\mathbf{V}) - \mathcal{F}\mathcal{N}\mathcal{F}(\mathcal{F}_K\mathbf{V})) = \mathcal{F}(\mathcal{N}\mathcal{F}_K - \mathcal{N}\mathcal{F})\mathbf{V} \; , \tag{5}$$

where $\mathcal{F}_K$ is a filtering operator with a filter width equal zero. In (5) only the standard operator occurs which acts on two solutions with different filter widths.

Let $\mathcal{F}_1 = \mathcal{F}$ and $\mathcal{F}_j$ filter operators with filter widths between these of $\mathcal{F}_K$ and $\mathcal{F}_1$. Equation (5) can be expanded into a sum of K operators

$$\mathcal{F}_1(\mathcal{N}\mathcal{F}_K - \mathcal{N}\mathcal{F}_1)\mathbf{V} = \mathcal{F}_1 \sum_{j=1}^{K} (\mathcal{N}\mathcal{F}_{j+1} - \mathcal{N}\mathcal{F}_j)\,\mathbf{V}\ . \tag{6}$$

To construct the approximate model operator we assume that the influence of each operator gets smaller with smaller filter width and the relation between adjacent operators is fixed for equally spaced filter widths. These assumptions are based on the power law in the inertial range. The second assumption can be formulated as

$$(\mathcal{N}\mathcal{F}_{j+1} - \mathcal{N}\mathcal{F}_j)\mathbf{V} = w(\mathcal{N}\mathcal{F}_j - \mathcal{N}\mathcal{F}_{j-1})\mathbf{V} \tag{7}$$

with a constant weight w. Applying (7) on (6) and even for one coarser filter width $\mathcal{F}_0$ we obtain

$$\mathcal{H}\mathcal{F}_1\mathbf{V} = \mathcal{F}_1 \sum_{j=1}^{K} w^j\,(\mathcal{N}\mathcal{F}_1 - \mathcal{N}\mathcal{F}_0)\,\mathbf{V}\ , \tag{8}$$

where the operation $\mathcal{F}_1(\mathcal{N}\mathcal{F}_0\mathbf{V})$ is interpreted as a local reconstruction of the evolution of the coarse solution according to the fluctuations of the fine solution. The mode of operation of the model can be explained as follows: It builds up a short history of the low modes and, out of the structure of the wave-number band between coarse and fine solution, the complete high-wave number information is extrapolated.

Since we are not interested in the error between exact and discretised solution but only in the difference between approximated DNS and LES solution, we consider a numerical method which is convergent of order p. Let $\mathcal{N}_D$ be the fully discretised operator of this method with the DNS solution $\mathbf{V}^n$ such that $\mathbf{V}^{n+1} = \mathcal{N}_D\mathbf{V}^n$. We now consider two solutions on two different grid levels L_0 and L_1. Let $\mathcal{F}_{L_1}$ be the LES filter operator and $\mathcal{F}_{L_0}$ a test filter which is twice as coarse. If we exchange the operators $\mathcal{N}$ through $\mathcal{N}_D$ in (8) we obtain as approximated modelling term

$$\mathcal{H}_D\mathcal{F}_{L_1}\mathbf{V}^n = w_K w_D(\mathcal{N}_D\mathcal{F}_{L_1} - \mathcal{N}_D\mathcal{F}_{L_0})\mathbf{V}^n\ , \tag{9}$$

with $w_K = \sum_{j=1}^{K} w^j$ and w_D is a weight which, in addition, takes the numerical viscosity into account.

A further question which is often neglected is the filtering in time. If the maximum time step is used, which is numerically allowed for the convective part (CFL $= O(1)$), the time evolution still contains the complete structures of the filtered solution. Hence, we determine the time step Δt on L_1 and calculate two steps on this level and one step with time step $2\Delta t$ on level L_0. In the filtered Navier-Stokes equations (2) the vector of the conserved quantities $\mathbf{U}$ is equal to $(\mathcal{F}_{L_1}\mathbf{V})$. Using equation (9) the filtered Navier-Stokes equations can be written (omitting the subscripts D and setting $\omega = w_K w_D$) as

$$\mathbf{U}^{n+1} = \mathcal{N}^2_{\Delta t} + \omega(\mathcal{N}^2_{\Delta t} - \mathcal{N}^1_{2\Delta t})\mathbf{U}^n \ ,$$

where Δt is the time step size and the superscripts denote the number of operations. Afterwards, this solution is filtered and projected onto the coarse grid. The efficiency of this model is dependent on the dimension of the problem. In two dimensions the additional CPU time is about 13% and in three dimensions about 7%, plus the time for evaluating the additional equation for $\overline{\rho}\hat{k}$ on the fine level. Therefore it is comparable with standard models.

In the limit of laminar flows (without discontinuities) the residual between the two operators becomes a term of order $p+1$ and will no longer influence the solution. The same argument holds in the limit of increasing numerical resolution, the so-called DNS limit, where the solution is smooth, because, for the numerical scheme, the resolved field behaves laminar and, again, the residual will become a term of order $p+1$, so that the model switches off automatically.

2.1 The weighting factors

2.1.1 Derivation of weight w_K

As mentioned above, we use the existence of a power law with a fixed decay α in the inertial range to estimate w. The mean value of a quantity f above a wave-number n can be approximated as

$$f_{n_j} = \int_{n_j}^{n_K} A\nu^{-\alpha} d\nu = \frac{A}{\alpha - 1}(n_j^{1-\alpha} - n_K^{1-\alpha}) \ , \quad (\alpha > 1) \ , \tag{10}$$

where n_j is the highest wave-number resolved for the filter $\mathcal{F}_j$. Combining equation (10) for two wave-numbers n_i and n_j ($n_i < n_j$) we get

$$f_{n_j} = f_{n_i} \left(\frac{n_i}{n_j} \right)^{\alpha-1} = \beta f_{n_i} \ . \tag{11}$$

Now we apply these global properties locally to each cell. Since we consider in (7) the time evolution of two adjacent ranges we choose $w = \beta$ and obtain

$$w_K = \beta \frac{\beta^K - 1}{\beta - 1} \ . \tag{12}$$

Since β is constant also w_K is fixed. In (11) β describes the ratio of two subgrid values for different wave-numbers. Since the subgrid kinetic energy $\overline{\rho}\hat{k}$ is known on both levels, the ratio of these values can be used to calculate a dynamic weight w_K. To ensure the conservation property the weight has to be fixed for each time-step, so that the values integrated over the whole domain Ω will be used to calculate the ratio

$$\beta = \int_\Omega \frac{(\overline{\rho}\hat{k})_{L_1}}{(\overline{\rho}\hat{k})_{L_0}} d\vec{\mathbf{x}} \ .$$

2.1.2 Derivation of weight w_D

In (9) an additional factor w_D has been introduced. The theoretical maximum wave-number of the LES solution which depends on the numerical mesh is $n_m = \frac{\Lambda}{2\Delta x}$ with the reference length Λ and grid spacing Δx. Due to the numerical viscosity the scales will be only resolved correctly up to a wave-number n_r. The weight w_D takes into account this numerical viscosity of the high modes between wave-numbers n_r and n_m. Typical spectrums for two under-resolved solutions E_0 and E_1 (here: the numerical viscosity is larger than the subgrid dissipation) are shown in a log-log plot in figure 1 together with a fully resolved spectrum E_K up to the Kolmogorov wave-number.

The difference between the two scales has to be calculated for our model. Then, for a fully resolved solution, this difference is equal to the shaded area I plus III in figure 1

$$\Omega_1 = \int_{\frac{1}{2}n_m}^{n_m} E_K(n) dn \ .$$

However, due to the numerical viscosity, the value is proportional to the area

$$\Omega_2 = \int_{\frac{1}{2}n_r}^{n_m} E_1 dn - \int_{\frac{1}{2}n_r}^{\frac{1}{2}n_m} E_0 dn$$

which are the shaded area II plus III of figure 1. The weight w_D is set as the ratio between these areas

$$w_D = \frac{\Omega_1}{\Omega_2} .$$

and has to be determined numerically for each method.

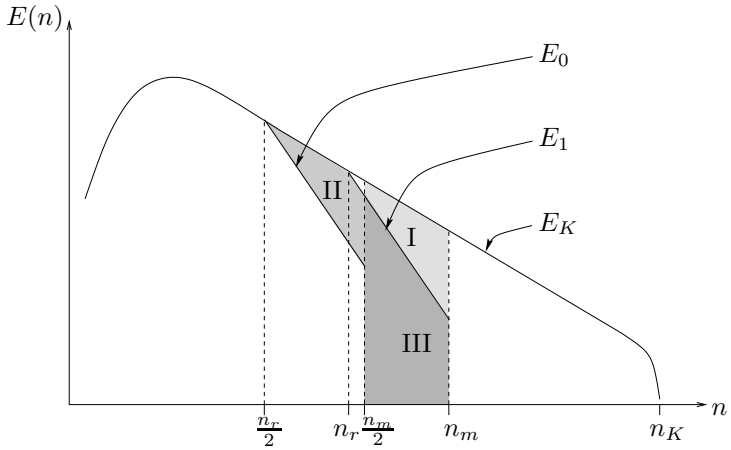

Figure 1: Sketch of typical spectra for a DNS (E_K) and two under-resolved solutions (E_1 and E_0)

2.2 The source term for the subgrid kinetic energy

In equation (3) we will neglect the pressure dilatation term

$$\overline{\vec{\mathbf{u}}^T \nabla p} - \tilde{\vec{\mathbf{u}}}^T \nabla \overline{p}$$

because it is not easy to model. However, this term is responsible for the exchange of internal energy and subgrid kinetic energy. To take this effect into account we have introduced a source term `s`. In two dimensions it is a

sink representing the dissipation that drives the subgrid kinetic energy during a relaxation time τ to an equilibrium value $(\overline{\rho}\hat{k})^{\mathrm{eq}}$

$$\mathsf{s} = \frac{(\overline{\rho}\hat{k})^{\mathrm{eq}} - (\overline{\rho}\hat{k})}{\tau} \ .$$

To estimate the equilibrium value and the relaxation time we use Obuchow's theory, where it is assumed that in the inertial range the flux of kinetic energy is constant and proportional to the cascading kinetic energy divided by a characteristic local time τ of the cascade. In [13] τ is considered as an eddy-turnover time

$$\tau = \frac{L}{v} \ ,$$

where L is the size of an eddy and v a typical velocity difference across the eddy

$$v = ||\mathbf{u}(\mathbf{x}) - \mathbf{u}(\mathbf{x} + \mathbf{n}_i|\Delta\vec{\mathbf{x}}|)||_2 \ ,$$

where $\mathbf{n}_i$ are normal vectors. The length L is related to the size of the frequency range $n_m \to 2n_m$ and thus, related to the filter width and therefore to the grid spacing

$$L = 2|\Delta\vec{\mathbf{x}}| \ .$$

The cascading kinetic energy itself is given as the difference $(\overline{\rho}\hat{k}) - (\overline{\rho}\hat{k})^{\mathrm{eq}}$. To influence the source term by the GS part, we determine the equilibrium value out of $(\overline{\rho}\hat{k})^{L_0}$, $(\overline{\rho}\hat{k})^{L_1}$ and using equations (11) and (12)

$$(\overline{\rho}\hat{k})^{\mathrm{eq}} = C_{\mathrm{eq}} \frac{\overline{\rho}v^2}{2} \frac{\beta^2}{1-\beta} \ .$$

The constant C_{eq} has to be obtained from comparisons with DNS solutions.

The source term described above is just a sink which accounts for the backscatter effect and can be applied in this form only to the two-dimensional case. In three space dimensions the cascading energy transfer from the low to the high modes is much more important and the source term must be also a source of subgrid kinetic energy. To obtain this term one can use a balance argument between total local dissipation and the resolved-scale viscous dissipation with the local GS energy production (see e. g. [10]).

3 Results

The model is validated on a freely decaying two-dimensional compressible turbulent flow. To obtain a reference solution a two-dimensional DNS is performed with initial conditions taken from [3] with a Reynolds number of 2000 and a reference Mach number of 0.3. The initial level of compressibility was chosen as 0.9 and the fluctuating r.m.s. levels of the velocities and the temperature as 0.1. Since the flow field is randomly initialised with a prescribed spectrum but uncorrelated phases a DNS with 512×512 points was calculated for the period of the acoustic transient (up to $t = 2$) so that the correlations are fully developed. This solution was filtered and used as initial values for the LES and under-resolved DNS calculations.

In the first step we determine w_D from two under-resolved DNS solutions. Therefore, we calculate one time step with a time step size Δt on a mesh with 64×64 and two time steps with $\frac{\Delta t}{2}$ on a mesh with 128×128 points. The ratio of the integrals Ω_1 to Ω_2 yields $w_D \approx 0.23$ for our second order method ($p = 2$), cf. [5], [6], [9]. For $\alpha = 3$ the fixed weight w_K results in

$$\lim_{K \to \infty} w_K = \frac{1}{3} \, .$$

We now examine the behaviour of the model for different grid resolutions. The residual of the modelling terms between two solutions will be computed in the L_1-norm. We expect that within the inertial range the model term should be locally of order $O(\Delta t^2)$ which corresponds to a diffusion of subgrid values and in the DNS limit it should be of $O(\Delta t^3)$ due to the numerical truncation error. If the LES solution is under-resolved the modelling term cannot be expected to give a reasonable value and the error will be large. We perform three successive calculations starting with one time step on a grid with 32×32 points (16×16 points for the test-filtered solution). For each of the following calculations the time step size and the grid spacing will be bisected and the number of time steps will be doubled. The source term has been switched off here. Table 1 shows the global order of the modelling term. For a too coarse resolution (32×32) the error is very large but within the inertial range (64×64 to 128×128) the model gives a second order correction (global order 1) and tends to a third order term in the DNS limit. Yet, the LES model is closed and two runs on a grid with 64×64 points are carried out. In the first run, we use the constant weight w_K and in the second, the dynamic weight is applied. These solutions will be compared with the DNS

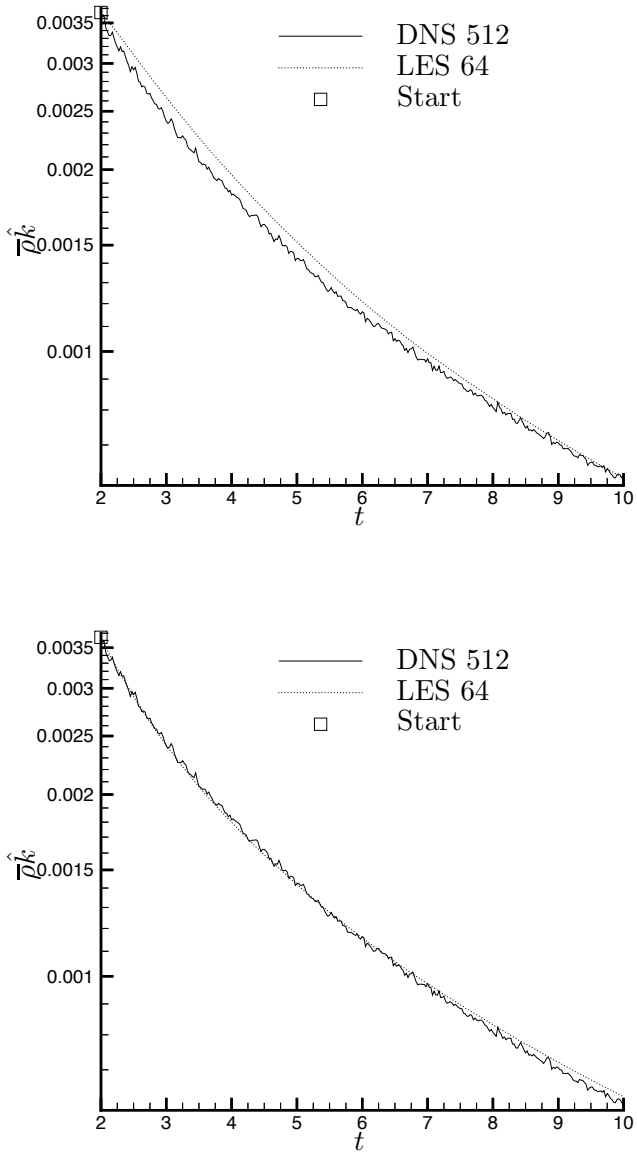

Figure 2: Time evolution of mean values of $\overline{\rho}\hat{k}$ (constant and dynamic weight w_K)

Resolution		Residual			Order		
L_1	L_0	ρu_1	ρu_2	ρE	ρu_1	ρu_2	ρE
32×32	16×16	2.77e-2	3.01e-2	1.91e-1			
64×64	32×32	2.45e-2	2.57e-2	1.78e-1	0.18	0.23	0.10
128×128	64×64	1.34e-2	1.39e-2	1.34e-1	0.88	0.89	0.41
256×256	128×128	5.19e-3	5.63e-3	7.67e-2	1.36	1.30	0.81
512×512	256×256	1.25e-3	1.42e-3	1.70e-2	2.06	1.99	2.17

Table 1: Global order of modelling term

solution on 512×512 (DNS 512) and an under-resolved DNS solution on 64×64 points (DNS 64).

To check the source term we compare the temporal evolution of the mean of the turbulent kinetic energy between the LES and the DNS 512 solution filtered on a 64×64 grid. We have set $C_{\text{eq}} = 2.75$ in the case of constant w_K and $C_{\text{eq}} = 1.75$ for the dynamic w_K. Figure 2 shows that the source term gives the qualitatively correct dissipation of the SGS kinetic energy.

The LES should recover the GS values of a filtered DNS solution. Therefore, we compare the mean value of the GS kinetic energy and the pressure versus time. For the first run, with constant weight w_K, an improvement of the LES solution compared with the under-resolved solution can be observed. With the use of the dynamic weight w_K in the second run, the LES solution recovers the kinetic energy very well for the whole simulation (see figure 3). The reproduction of the pressure is also good up to time 6 but afterwards the two solutions disperse (see figure 4). Nevertheless, the quality of the solution of the second run is better than that of the first run.

The spectra of the kinetic energy for the two DNS and the LES solution at times $t = 5$ and $t = 10$ are shown in figures 5 and 6 for both runs. In all cases the LES solutions recover the spectra up to wave-number $n_r \approx 10$ for the whole simulation, while the under-resolved DNS solution gets continuously worse in time. The overprediction of the spectra of the LES solution between wave-numbers 10 and 14 is probably a result of the backscatter-effect, where the SGS kinetic energy forces the GS kinetic energy. The constant value of $n_r \approx 10$ indicates that the number of grid points required to resolve one wave-length is about 7 for this setting, which is a good result for a second order scheme.

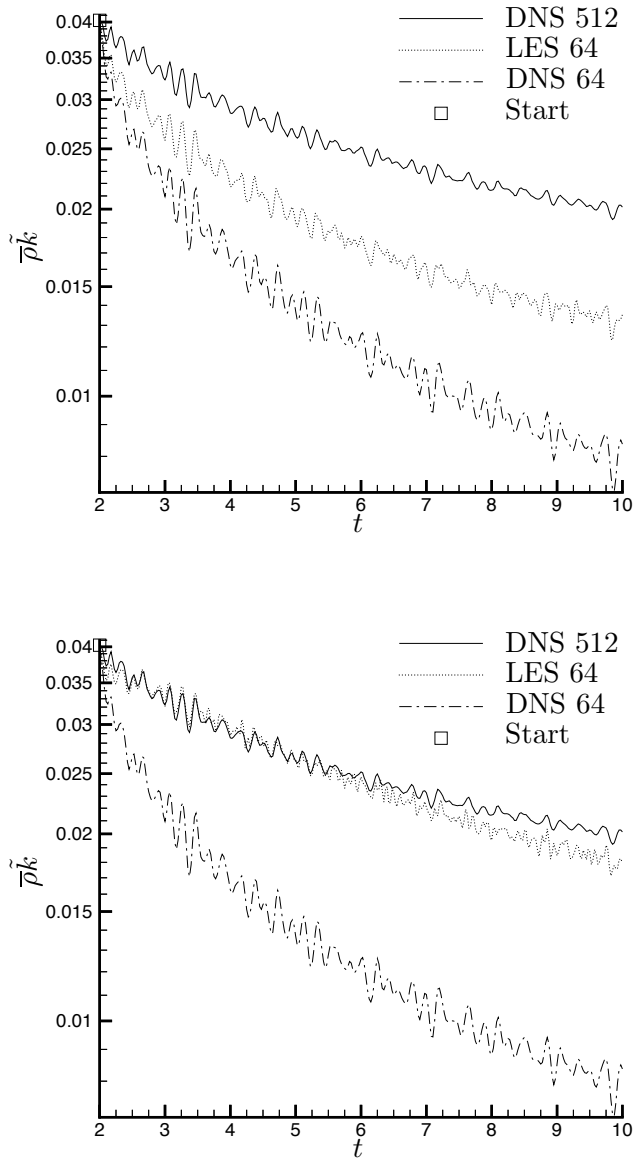

Figure 3: Time evolution of mean values of $\overline{\rho}\tilde{k}$ (constant and dynamic weight w_K)

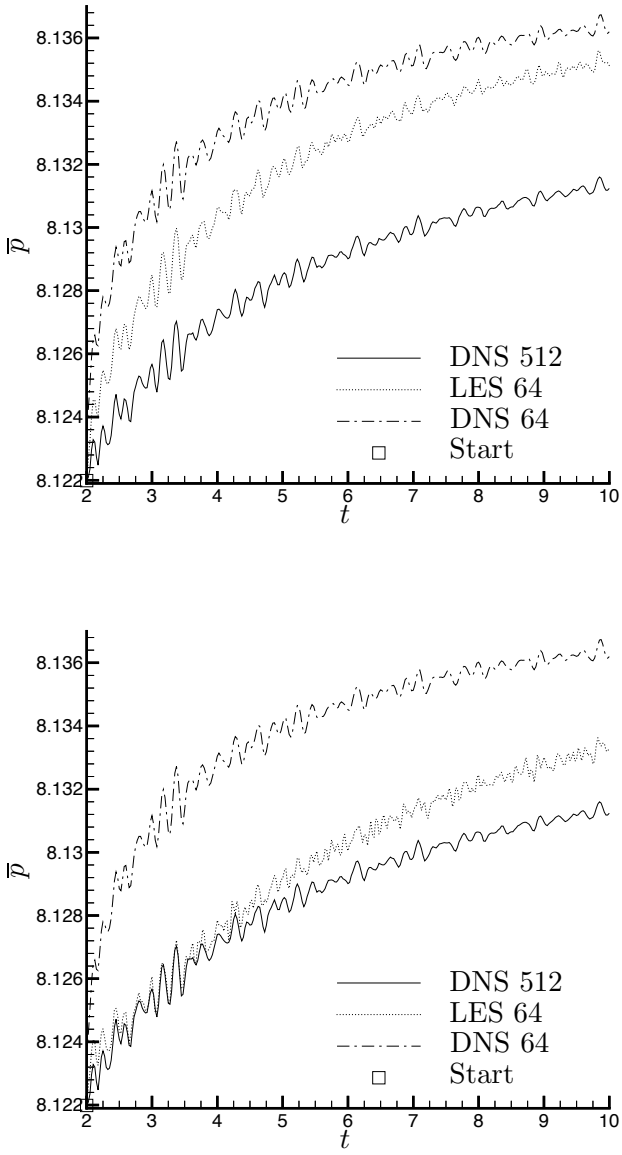

Figure 4: Time evolution of mean values of $\overline{p}$ (constant and dynamic weight w_K)

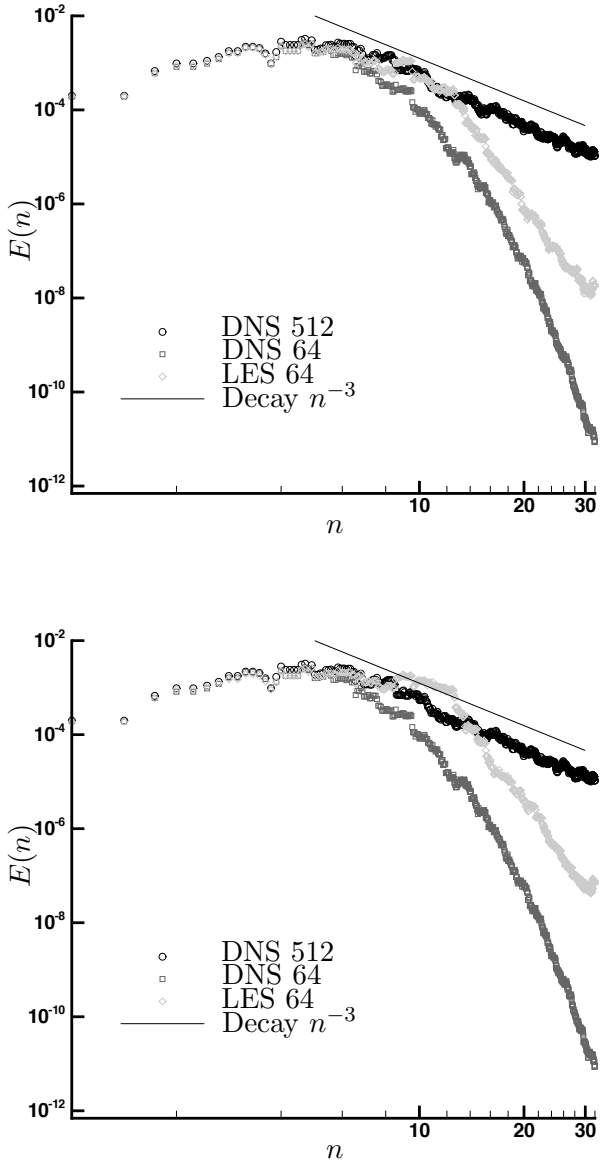

Figure 5: Kinetic energy spectrum at $t = 5$ (constant and dynamic weight w_K)

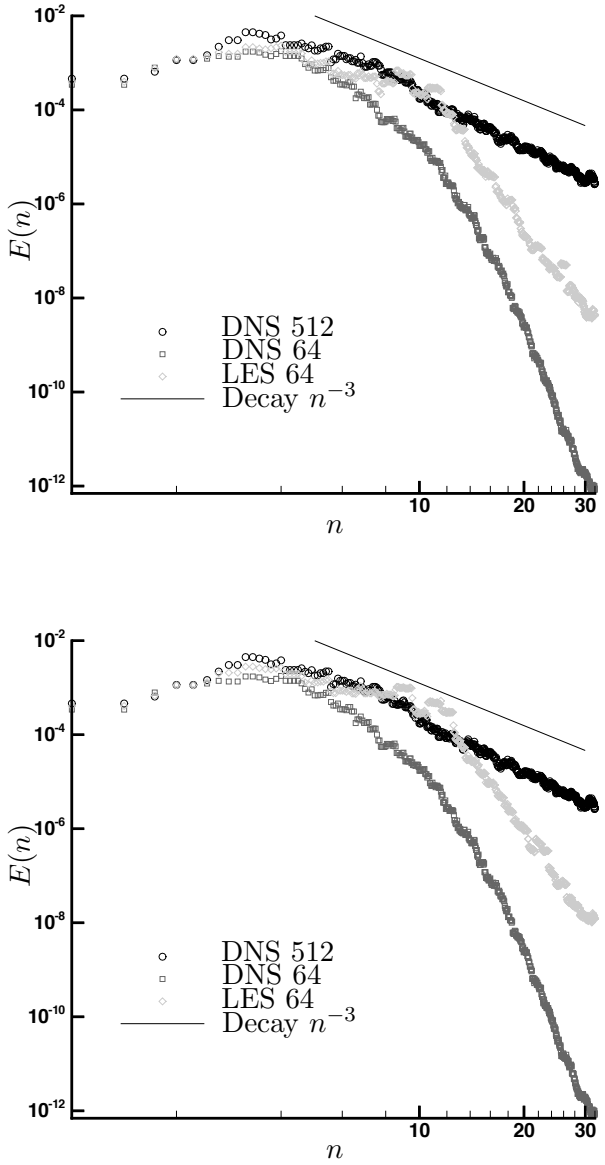

Figure 6: Kinetic energy spectrum at $t = 10$ (constant and dynamic weight w_K)

References

[1] J. P. Boris, F. F. Grinstein, E. S. Oran and R. L. Kolbe. New insights into large eddy simulation. *Fluid Dynamics Research*, 10:199–228, 1992.

[2] G. L. Browning, W. D. Henshaw and H.-O. Kreiss. A numerical investigation of the interaction between the large and small scales of the two-dimensional incompressible Navier-Stokes equations. Technical Report 98-23, Computational and Applied Mathematics, Univ. of California, Los Angeles, April 1998.

[3] G. Erlebacher, M. Y. Hussaini, H. O. Kreiss and S. Sarkar. The analysis and simulation of compressible turbulence. *Theor. Comput. Fluid Dynamics*, 2, 1990.

[4] G. Erlebacher, M. Y. Hussaini, C. G. Speziale and T. A. Zang. Toward the large-eddy simulation of compressible turbulent flows. *J. Fluid Mech.*, 238, 1992.

[5] M. Fey. Multidimensional upwinding, Part I: The method of transport for solving the Euler equations. *J. Comp. Phys.*, 143:159–180, 1998.

[6] M. Fey. Multidimensional upwinding, Part II: Decomposition of the Euler Equations into advection equations. *J. Comp. Phys.*, 143:181–199, 1998.

[7] A. Leonard. On the energy cascade in large-eddy simulations of turbulent fluid flows. *Adv. Geophys.*, 18A:237–248, 1974.

[8] M. Lesieur and P. Compte. Large-eddy simulations of compressible turbulence flows. In *Turbulence in compressible flows*, AGARD Report No. 819, 1997.

[9] J. Maurer. The Method of Transport for mixed hyperbolic-parabolic systems. Research Rep. 97-13, Sem. for Applied Mathematics, ETH Zurich, 1997.

[10] A. Misra and D. I. Pullin. A vortex-based subgrid stress model for large-eddy simulation. *Phys. Fluids*, 9(8):2443–2454, 1997.

[11] Y. Morinshi, T. S. Lund, O. V. Vasilyev and P. Moin. Fully conservative higher order finite difference schemes for incompressible flow. *J. Comp. Physics*, 143:90–124, 1998.

[12] U. Piomelli, W. H. Cabot, P. Moin and S. S. Lee. Subgrid-scale backscatter in turbulent and transitional flows. *Physics of Fluids*, 3(7):1766–1771, 1991.

[13] H. A. Rose and P. L. Sulem. Fully developed turbulence and statistical mechanics. *Journal de Physique*, 39(5):441–484, 1978.

Research Reports

No.	Authors	Title
99-06	J. Maurer, M. Fey	A Scale-Residual Model for Large-Eddy Simulation
99-05	M.J. Grote	Am Rande des Unendlichen: Numerische Verfahren für unbegrenzte Gebiete
99-04	D. Schötzau, C. Schwab	Time Discretization of Parabolic Problems by the hp-Version of the Discontinuous Galerkin Finite Element Method
99-03	S.A. Zimmermann	The Method of Transport for the Euler Equations Written as a Kinetic Scheme
99-02	M.J. Grote, A.J. Majda	Crude Closure for Flow with Topography Through Large Scale Statistical Theory
99-01	A.M. Matache, I. Babuška, C. Schwab	Generalized p-FEM in Homogenization
98-10	J.M. Melenk, C. Schwab	The hp Streamline Diffusion Finite Element Method for Convection Dominated Problems in one Space Dimension
98-09	M.J. Grote	Nonreflecting Boundary Conditions For Electromagnetic Scattering
98-08	M.J. Grote, J.B. Keller	Exact Nonreflecting Boundary Condition For Elastic Waves
98-07	C. Lage	Concept Oriented Design of Numerical Software
98-06	N.P. Hancke, J.M. Melenk, C. Schwab	A Spectral Galerkin Method for Hydrodynamic Stability Problems
98-05	J. Waldvogel	Long-Term Evolution of Coorbital Motion
98-04	R. Sperb	An alternative to Ewald sums, Part 2: The Coulomb potential in a periodic system
98-03	R. Sperb	The Coulomb energy for dense periodic systems
98-02	J.M. Melenk	On n-widths for Elliptic Problems
98-01	M. Feistauer, C. Schwab	Coupling of an Interior Navier–Stokes Problem with an Exterior Oseen Problem
97-20	R.L. Actis, B.A. Szabo, C. Schwab	Hierarchic Models for Laminated Plates and Shells
97-19	C. Schwab, M. Suri	Mixed hp Finite Element Methods for Stokes and Non-Newtonian Flow
97-18	K. Gerdes, D. Schötzau	hp FEM for incompressible fluid flow - stable and stabilized
97-17	L. Demkowicz, K. Gerdes, C. Schwab, A. Bajer, T. Walsh	HP90: A general & flexible Fortran 90 hp-FE code